

Effects of vertical component of near-field ground motions on seismic responses of asymmetric structures supported on TCFP bearings

Nasim Partovi Mehr^{1a}, Faramarz Khoshnoudian^{*1} and Hamed Tajammolian^{2b}

¹Faculty of Civil Engineering, Amirkabir University of Technology (Tehran Polytechnic), Tehran, Iran

²Faculty of Civil Engineering, Yazd University, Yazd, Iran

(Received December 11, 2016, Revised November 19, 2017, Accepted November 25, 2017)

Abstract. The effects of vertical component of earthquakes on torsional amplification due to mass eccentricity in seismic responses of base-isolated structures subjected to near-field ground motions are studied in this paper. 3-, 6- and 9-story superstructures and aspect ratios of 1, 2 and 3 have been modeled as steel special moment frames mounted on Triple Concave Friction Pendulum (TCFP) bearings considering different period and damping ratios. Three-dimensional linear superstructures resting on nonlinear isolators are subjected to both 2 and 3 component near-field ground motions. Effects of mass eccentricity and vertical component of 25 near-field earthquakes on the seismic responses including maximum isolator displacement and base shear as well as peak superstructure acceleration are studied. The results indicate that the effect of vertical component on the responses of asymmetric structures, especially on the base shear is significant. Therefore, it can be claimed that in the absence of the vertical component, mass eccentricity has a little effect on the base shear increase. Additionally, the impact of this component on acceleration is remarkable so the roof acceleration of a nine-story structure has been increased 1.67 times, compared to the case that the structure is subjected to only horizontal components of earthquakes.

Keywords: TCFP isolators; near-field earthquakes; eccentricity; vertical component; steel frames

1. Introduction

Base isolation system is an acceptable approach to lessen displacement and acceleration of structures by isolating the superstructures from the earthquakes. In this way, by reducing input energy of superstructure and controlling the responses of it, the structural and non-structural damages during severe ground shakings are significantly decreased. Increasing the stiffness, ductility and energy dissipation of the structures can control these responses. Reducing structural damages will sustain the operational performance level of the building, so base isolating is a desirable way for protecting structures with high importance occupancy through a ground motion.

Despite many researchers have investigated several base isolation systems, they can be categorized in two main types: elastomeric and frictional bearings. Three groups of Frictional bearings are introduced as Single Friction Pendulum (SFP), Double Concave Friction Pendulum (DCFP) and Triple Concave Friction Pendulum (TCFP) bearings. The section of a TCFP isolator can be seen in Fig. 1(a). It consists of four concave plates separated by a nested slider in the middle of them. The bottom and top sliding

edges are named as 1, 2, 3 and 4 respectively. Whereas the radius of each sliding plate denotes R_i and its displacement capacity stands for d_i . The sliding plates are covered by a non-metallic material with friction coefficient of μ_i . By utterly adjustment of radii and friction coefficients of plates, a 5-regime backbone curve can be obtained that is shown in Fig. 1(b) (Loghman *et al.* 2015a).

Comparing with SFP and DCFP bearings which have bilinear and tri-linear behaviors respectively, TCFP bearing has the hardening regimes at the end of its backbone curve, i.e., regimes IV and V in Fig. 1(b), which improves the reliable performance of it. Tajammolian *et al.* (2014) have declared that TCFP bearing experiences smaller displacement in comparison with SFP and DCFP isolators exerted to simplified pulses of near-field ground motions.

Many researches have presented an adaptive model for predicting the seismic behavior of a TCFP bearing. The first model has been introduced by Fenz and Constantinou (2008a,b). They idealized the adaptive behavior of the TCFP isolator by using three SFP elements connected in series. In this study, we have utilized this model for estimating seismic performance of base-isolated structures with TCFP bearings. Hence, extensive explanation will be presented in chapter 2. Becker and Mahin (2012, 2013) have presented another model for predicting the responses of the TCFP isolated structures subjected to bi-directional ground motions. Dao *et al.* (2013) have modified the series model introduced by Fenz and Constantinou by adding a circular gap element to them, so the new model can simulate three-dimensional behavior of base-isolated structures isolating with TCFP bearings. They have verified their proposed model with experimental tests and have

*Corresponding author, Professor
E-mail: khoshnud@aut.ac.ir

^aMsc Graduate
E-mail: n.partovimehr@aut.ac.ir

^bAssistant Professor
E-mail: h.tajammolian@yazd.ac.ir

implemented the TCFP isolator element in OpenSees software. For predicting real behavior of TCFP bearing in uplift conditions, Sarlis and Constantinou (2013) have improved the formulations of force-displacement equations. Fadi and Constantinou (2010) analyzed TCFP bearings using simplified methods presented by the current structural codes. They described the tools for the simple analyses of this type of seismically isolated structures using abundant nonlinear response history analysis results. They concluded that simplified methods of analysis systematically estimated good and often conservative isolator displacement demands and they provided good evaluations of isolator peak velocities. In their study, effect of vertical component of earthquakes were neglected. Yurdakul and Ates (2011) studied the effectiveness of TCFP modeled by a series arrangement of the three single concave friction pendulum (SCFP) on a two-dimensional eight-story building. They concluded that the TCFP bearings are more effective than different types of isolation bearings for isolating the structures against severe ground motions. Ates and Yurdakul (2011) also evaluated the site-response effects on the aforementioned buildings. They investigated the isolated systems on soft, medium and firm soil and declared that the site-response had significant effects on their response.

The performance of base-isolated structures mounted on TCFP bearings subjected to the earthquakes with various intensity levels in different damage states have been studied by Morgan and Mahin (2010, 2011). Tajammolian *et al.* (2014) scrutinized the responses of a Single Degree of Freedom (SDF) superstructure resting on TCFP bearings subjected to simplified forward directivity and fling step pulse models. Jangid and Kelly (2001) investigated the responses of superstructures mounted on different elastomeric isolators that were subjected to six pairs of horizontal components of near-fault records. Jangid (2005) declared that controlling the responses of a structure subjected to near-fault ground motions requires optimum friction coefficient in the range of 0.05 to 0.15 in SFP isolators. Variable Friction Pendulum System (VFPS) which improved the performance of the SFP isolator in near-fault motions is suggested by Panchal and Jangid (2008). Dicleli (2007) and Dicleli and Buddaram (2007) did research on use of isolators with bilinear backbone curve in protection of bridges against near-field ground motions. Researchers have investigated the effects of earthquakes regardless of torsion, on seismic responses of isolated structures mounted on SFP, DCFP and TCFP bearings (Khoshnoudian and Rezai Haghdoost 2009, Rabiei and Khoshnoudian 2013, Loghman and Khoshnoudian 2015, Loghman *et al.* 2015b, Tajammolian *et al.* 2016a,b).

Kilar and Koren (2009) have introduced two types of eccentricities that should have been considered in torsional coupled base-isolated structures: mass eccentricity in superstructure and stiffness eccentricity in isolators. The fact that SFP isolators contribute to control the torsional responses of one-story structures with mass eccentricity has been demonstrated by Zayas *et al.* (1987, 1989). Almazan and de la Llera (2003) assessed the effects of accidental eccentricity caused by overturning on the seismic response

of symmetric structures mounting on SFP bearings. They also conducted some experimental tests concluding mass eccentricity can increase the isolator displacement up to 6% in 3-story isolated structures (De la Llera and Almazan 2003).

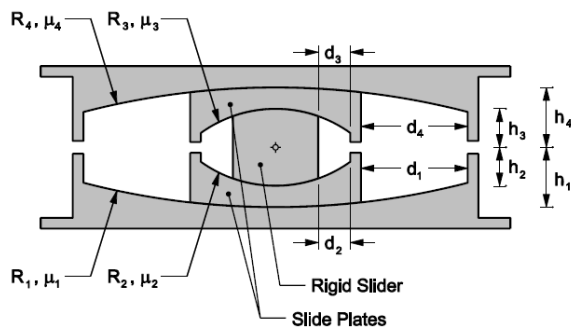
Diverse distributions of Center of Mass (CM) in the superstructure and Center of Stiffness (CS) of LRB isolators have been scrutinized by Kilar and Koren (2009). They illustrated that while CS is moved into the mirror position of CM (i.e., $CS = -CM$), the isolator displacement may get enlarged up to 1.4 comparing with the symmetric case ($CS = CM$) under bidirectional far-field ground motions.

Tena-Colunga and Gomez-Soberon (2002) did study on torsional responses of base-isolated structures with mass eccentricity. Torsional effects of base-isolated structures with elastomeric bearings when eccentricity occurs both in the superstructure and isolator were investigated by Tena-Colunga and Escamilla-Cruz (2007). They declared that torsional amplifications in the bearing displacement in the superstructure with mass eccentricity are greater than the amplifications regardless of stiffness eccentricity of the isolators. Tena-Colunga and Zambrana-Rojas (2006) studied effect of eccentricities in isolators using a bilinear isolation system subjected to unidirectional and bidirectional actions of selected ground motions.

Khoshnoudian and Imani Azad (2011) investigated effects of both mass eccentricity of a superstructure and stiffness eccentricity of isolators on the superstructure and isolator itself. They demonstrated that bidirectional near-fault ground motions would magnify torsional intensification in comparison with unidirectional ones in a bilinear isolation system. Torsional responses of base-isolated structures subjected to different ground motions have been investigated by De la Llera and Chopra (1994), Jangid and Datta (1995) Ryan and Chopra (2006), Picazo *et al.* (2015) and Siringurino and Fujino (2015). Tajammolian *et al.* (2016a) have investigated the effect of mass eccentricity on the torsional behavior of structures subjected to structure subjected to three components of earthquake simultaneously. Otherwise, the error may be about 30%. They also illustrated that considering vertical component in calculations is important when the bearing displacement is remarkable.

Roussis and Constantinou (2006a,b) studied the effect of vertical component of ground motion on XY-FP isolators. The XY-FP isolator is two orthogonal opposing concave beams interconnected within a sliding mechanism. They investigated the possibility of uplift occurrence on a five-story base-isolated structure resting on XY-FP isolators, using analytical and experimental researches. It was bidirectional component of earthquakes. In their study the role of vertical component of ground motion is ignored. The current paper is an attempt to fill this gap.

Seismic responses of single-degree-of-freedom (SDOF) and multiple-degree-of-freedom structures supported on a SFP isolator under three components of ground motions was investigated by Almazan *et al.* (1998). They demonstrated that the effect of the vertical component of an earthquake depends on the ratio of horizontal to vertical component of ground motions.



(a) TCFP isolator section (Fenz and Constantinou 2008a)

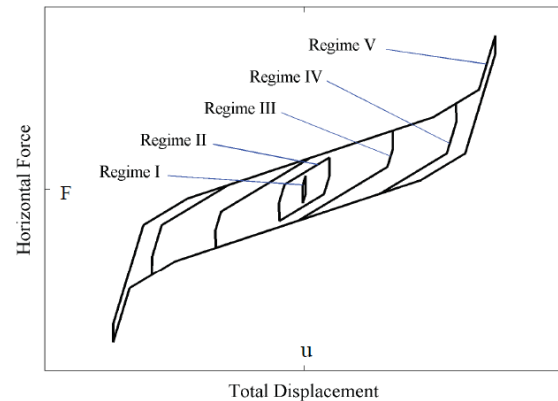
(b) Backbone curve of a TCFP (Constantinou *et al.* 2011)

Fig. 1

When this ratio is small (less than 0.15), ignoring the vertical component leads to a 15% error in base shear of the structure compared with a shown that the XY-FP isolation system is useful to prevent uplift in most extreme conditions such as excitation under near-fault strong ground motions and uplift-prone structural systems.

Rabiei and Khoshnoudian (2011) also investigated seismic responses of multi-story friction pendulum base-isolated structures under the vertical component of ground motion. Their research demonstrated that the maximum error caused by neglecting the vertical component of a ground motion in determining the peak bearing displacement, base shear and roof acceleration of the structure are 15.61%, 36%, and 50.12%, respectively.

They revealed that the effect of the vertical component of ground motion is significant for short and rigid structures with $T_s < 0.45s$ (T_s is the period of superstructure).

Effect of the vertical component of ground motion on the seismic responses of DCFP base-isolated structures was also studied by Khoshnoudian and Rabiei (2010). Their study demonstrated that the maximum error caused by neglecting the vertical component of ground motion on the peak bearing displacement and base shear of the isolated-structures were 5% and 22%, in the same order. It was illustrated that the error for base shear was considerable when the superstructure period declined. The effect of vertical component of near-fault earthquakes on the seismic responses of TCFP bearings was investigated by Loghman *et al.* (2015a). Their study showed that the maximum error caused by neglecting the vertical component of earthquake in determining the base shear of the structure was 29.5 percent and the error was negligible on the peak bearing displacement.

Although many investigations have been conducted in order to study the torsional behavior of base-isolated structures with elastomeric or SFP bearings, the seismic behavior of isolated structures with mass asymmetry mounted on TCFP bearings and subjected to three components of ground motion have not been addressed yet. Note, that considering the effect of vertical component of earthquake which can amplify the torsional behavior is a gap among existing investigation. As the base shear of

TCFP bearings depends on their vertical weight, it is expected to seriously be affected by vertical component of earthquake. 25 sets of three components near-fault ground motion record are used for this purpose. As discussed earlier, TCFP has a 5-regime backbone curve with hardening behavior in phases IV and V of the motion. Therefore, this hardening is expected to control the responses amplification due to torsion in TCFP base isolated structures, better than SFP and DCFP ones. Previous studies show that the effect of mass eccentricity in superstructure is much severe comparing with stiffness eccentricity of isolators; therefore, this kind of eccentricity is considered in current investigation. This study focuses on the torsional effects of near-fault excitations on the engineering demand responses, such as isolation displacement, base shear and roof acceleration of superstructures mounted on TCFP isolators. TCFP bearings with a reasonable range of effective periods and damping ratios are considered, while various slenderness (Height/Width) and aspect (Length/Width) ratios of superstructure are assumed.

2. TCFP modeling and design

Behaviour of TCFP isolator is more complicated than the other concave friction pendulum bearings because it has more sliding surfaces (Fig. 1). The behaviour has a backbone curve with five different phases of motion. In the regimes I to III, isolator displacement is in a softening manner while the curve slope changes in phases IV and V and develops stiffer. Entirely adaptive movement of the isolator will happen when the friction coefficients of sliding plates are $\mu_2 = \mu_3 < \mu_1 < \mu_4$. A method was proposed by Fenz and Constantinou (2008a) to simulate multi-spherical sliding isolators' behavior. In their method three SFP elements can be used for idealizing a TCFP model (Fig. 2). It should be noted that in spite of the fact that a TCFP is made up of four sliding surfaces, the two inner plates (surfaces 2 and 3 in Fig. 1(a)), commonly have similar radii and friction coefficients; hence they can be modeled by one SFP element. Furthermore, some gap elements are used in this model to simulate the hardening behavior of regimes IV

Table 1 Characteristics of ground motion records

No	Record	Station	Soil Type	Max. PGA (g)	Max. PGV (cm/s)	M_w
1	Cape Mendocino	Petrolia	C	0.662	82.1	7
2	Chi-Chi, Taiwan	TCU065	D	0.789	127.7	7.6
3	Chi-Chi, Taiwan	TCU068	D	0.507	191.1	7.6
4	Chi-Chi, Taiwan	TCU075	D	0.332	88.4	7.6
5	Coalinga-05	Oil City	C	0.841	41.2	5.8
6	Coalinga-05	Transmitter Hill	C	1.083	46.1	5.8
7	Duzce	Duzce	D	0.535	83.5	7.2
8	Duzce	Bolu	C	0.822	62.1	7.1
9	Erzican, Turkey	Erzincan	D	0.496	95.4	6.7
10	Imperial Valley-06	Elcentro#5	C	0.528	91.5	6.5
11	Imperial Valley-06	Elcentro#7	D	0.463	108.8	6.5
12	Imperial Valley-06	Elcentro#8	C	0.602	48.6	6.5
13	Kobe	Takatori	D	0.616	169.6	6.9
14	Kobe	Takarazuka	D	0.697	72.6	6.9
15	Kocaeli, Turkey	Gebze	B	0.261	52	7.5
16	Landers	Barstow	D	0.135	30.4	7.3
17	Landers	Lucerne	C	0.789	140.3	7.3
18	Loma Prieta	Oakland	D	0.29	49.2	6.9
19	Loma Prieta	Saratoga	C	0.512	55.6	6.9
20	Morgan Hill	Coyote Lake Dam	B	1.303	62.3	6.2
21	N. Palm Strings	North Palm Strings	D	0.693	73.6	6.1
22	Northridge-01	Sylmar-Converter Station	C	0.897	130.3	6.7
23	Northridge-01	Sylmar-Converter Station East	C	0.828	116.6	6.7
24	Northridge-01	Sylmar-Olive View	C	0.843	122.7	6.7
25	San Fernando	Pacoima Dam	B	1.24	116.5	6.6

and V. The series model was developed in SAP2000 software which the details can be referred to Fenz and Constantinou (2008b) study.

The restrainer of each sliding plate is assumed as almost rigid. This assumption is considered in most researches related to the modeling of TCFP bearings, e.g., Fenz and

Constantinou (2008a), Morgan and Mahin (2011) and Becker and Mahin (2012). The real stiffness of the restrainer part should be modified according to experimental examinations. In this study, the value is selected according to Fenz and Constantinou (2008a) assumptions. Also the properties of the TCFP isolator, i.e.,

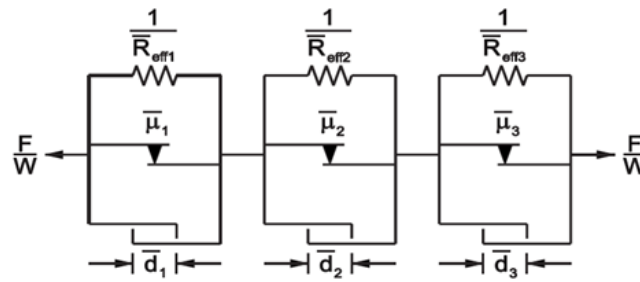


Fig. 2 Series model of TCFP isolator (Fenz and Constantinou 2008b)

R_1 to R_4 and μ_1 to μ_4 , should be modified for utilizing in the three-element series model. The formulas of this modification can be found in Fenz and Constantinou study (2008b).

The effective period (T_{eff}) and damping (ξ_{eff}) of the isolators are usually used in seismic codes as their design parameters. The appropriate equations to obtain these values in TCFP bearing were introduced by Becker and Mahin (2012). Different ranges of possible friction coefficients are reported in literature. Friction ranges have been identified as low, medium and high by Morgan and Mahin (2010) as 0.01 to 0.02, 0.05 to 0.08 and 0.1 to 0.2, respectively. This definition is also used in this investigation.

3. Earthquake selection

Near-fault ground motions have some distinguished characteristics that differ from far-fault seismic excitations. Two specifications of these ground motions are high-frequency component in acceleration records as well as long-period velocity pulses (Masaeli *et al.* 2014). Previous study showed that Peak Ground Velocity (PGV) is a crucial parameter for seismic responses of structures under near field earthquakes (Tajammolian *et al.* 2014). Consequently, twenty-five sets of ground motion records are selected as they included a reasonable range of PGVs from 30 to 190 cm/s (PEER 2013). It should be noted that the near-fault ground motions in which the period of the velocity pulse (T_p) is close to the isolator effective period (T_{eff}) may cause amplification in the responses (Khoshnoudian and Ahmadi 2013); however, the effective damping of the isolator will drop the influence of this amplification to some extent. Moreover, the utilized ground motions encompass a wide range of soil properties as well as Peak Ground Acceleration (PGA). Most of the utilized records have magnitude greater than 6. The records' specifications such as soil type, PGA, PGV and magnitude are presented in Table 1.

4. Design of superstructure

In order to investigate the effects of vertical component of ground motions and torsion on base-isolated structures, five superstructures are designed (Table 2). These five

Table 2 Properties of superstructures

No.	a (m)	b (m)	H (m)	$\beta=H/b$	$\gamma=a/b$
1	15	15	10	0.67	1
2	15	15	20	1.33	1
3	30	15	20	1.33	2
4	45	15	20	1.33	3
5	15	15	30	2.00	1

superstructures are selected to form a reasonable range of superstructure qualifications, i.e., aspect ratios and slenderness. As shown in Table 2, the aspect ratio of superstructures indicating of plan length to width ratio (a/b) is equal to 1, 2 and 3. Rectangular plans are considered as well as square ones. The slenderness ratio, i.e., structure height to plan width (H/b), is proposed as 0.67, 1.33 and 2.

The reference model in current study is the superstructure No. 2 in Table 2, which is illustrated in Fig. 3. This 6-story structure has three bays in length and in width. The length of each bay and the height of each story are 5 and 3.33 m, in the same order; thus, the total height of the reference superstructure is 20m.

According to ASCE 7-10 Dead and Live loads were selected as 8 and 4 kN/m² respectively. The seismic load was calculated by the Equivalent Lateral Force (ELF) method. Although the seismic analysis of the superstructure with more than 20 m height, i.e., structure No. 3, was checked using the Response Spectrum Procedure of ASCE 7-10 document (ASCE 7, 2010).

The superstructures have steel special moment frames as lateral resisting systems and designed using LRFD method of AISC Specifications for Structural Steel Buildings (AISC 360, 2010) and the design was confirmed with minimum requirements of AISC Seismic Provisions for Structural Steel Buildings (AISC 341, 2010). Box-type square sections and standard W-shape profiles were assumed for columns and beams, respectively. The proportioned sections of reference superstructure are shown in Fig. 3(d) as an example.

5. Effect of mass eccentricity

Three crucial engineering parameters are considered to study the effects of near-fault ground motions on the

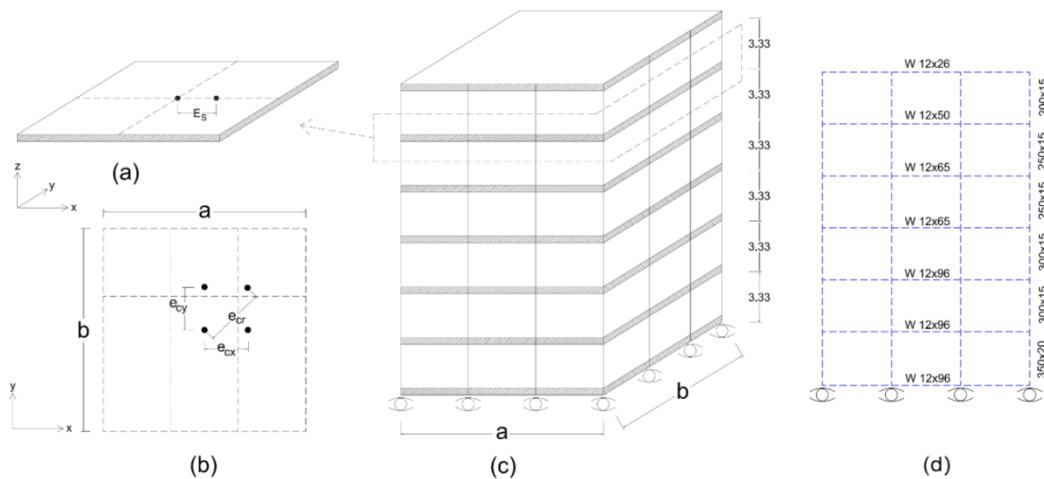


Fig. 3 (a) Mass eccentricity, (b) Plan of reference structure, (c) 3D model of reference structure and (d) Designed sections of reference structure

responses of base-isolated structures with TCFP bearings.

The parameters that have been investigated are maximum isolator displacement, base shear of structures and maximum roof acceleration of superstructures. The structures are subjected to the components of earthquakes both with and without the vertical component in addition to the transitional ones. The three-dimensional structure in Fig. 3 is subjected to 25 near-field earthquakes in both x - and y -direction. From here on, maximum isolator displacement and roof acceleration of the superstructure are written as isolator displacement and roof acceleration.

Three classifications of eccentricity are considered to highlight the role of superstructure mass eccentricity in.

To determine the impact of mass eccentricity of the superstructure, the peak amounts of base shear, isolator displacement and roof acceleration are selected as the main engineering demand parameters. "Amp. Factor" is defined as the ratio of response in the asymmetric model to the similar response in the symmetric structure according to Eq. (1) to facilitate the study in this section.

$$\text{Amp. Factor} = \frac{\text{RESPONSE (Asymmetric Model)}}{\text{RESPONSE (Symmetric Model)}} \quad (1)$$

All the structures presented in Table 2 are analyzed subjected to the components of earthquake records consist of two transitional ones with vertical component (XYZ case) and without it (XY case) in both symmetric and asymmetric models. Mean of peak values of calculated "Amp. Factor" among all results is calculated for each asymmetric model to illustrate the maximum effect of eccentricity clearly.

As the pattern of changes, in both x and y direction are almost identical and larger y -component amounts of earthquakes cause more increasing factors. Results of y -direction are given in the following three chapters (5.1, 5.2 and 5.3).

5.1 Aspect Ratio (γ)

Amplification factor of isolator displacement magnification of the responses of the base-isolated structure. All following types of eccentricity can be seen in Fig. 3(a).

- 1- Longitudinal eccentricity (e_{cx}) with the values of 5, 10, 15 and 20% of plan length (a).
- 2- Transversal eccentricity (e_{cy}) with the values of 5, 10, 15 and 20% of plan width (b).

Diagonal eccentricity (e_{cr}) with the values of 5, 10 and 15% of plan diagonal ($r = (a^2 + b^2)^{1/2}$).

in y -direction caused by mass eccentricity is shown in Fig. 4. All superstructures been used in this chapter have rested on isolators with effective period and damping ratio of 5 second and 15%, respectively. Results of the models subjected to XY components of ground motions are demonstrated in part (a) of the Fig. while part (b) graphs show the results of the models experiencing all three components of earthquakes (XYZ case). Note that in structures with γ equal to 2 and 3, 15% of mass eccentricity in diagonal direction causes instability in structure, so the results of this eccentricity case is not presented. As seen in the figure, mass eccentricity has not changed the displacement of isolator significantly. Maximum amplification factor of isolator displacement is obtained from the model with aspect ratio of 3 and longitudinal eccentricity of 20%. This peak value has been 1.068 in the presence of the vertical component (XYZ). According to the diagrams of the figure, increase in aspect ratio of structure has caused increase in isolator displacement. For instance, amplification factor of displacement in XYZ case for longitudinal eccentricity of 20% is 1.038, 1.047 and 1.068 for structures with aspects of 1, 2 and 3, in the same order. It is clear that with increase in length of structure and then escalation of its torsion arm, torsional effect of eccentricity increases.

The greatest impact of mass eccentricity on displacement is related to the direction perpendicular to the movement path that is longitudinal eccentricity (e_{cx}). Maximum amplification factors of the response in y

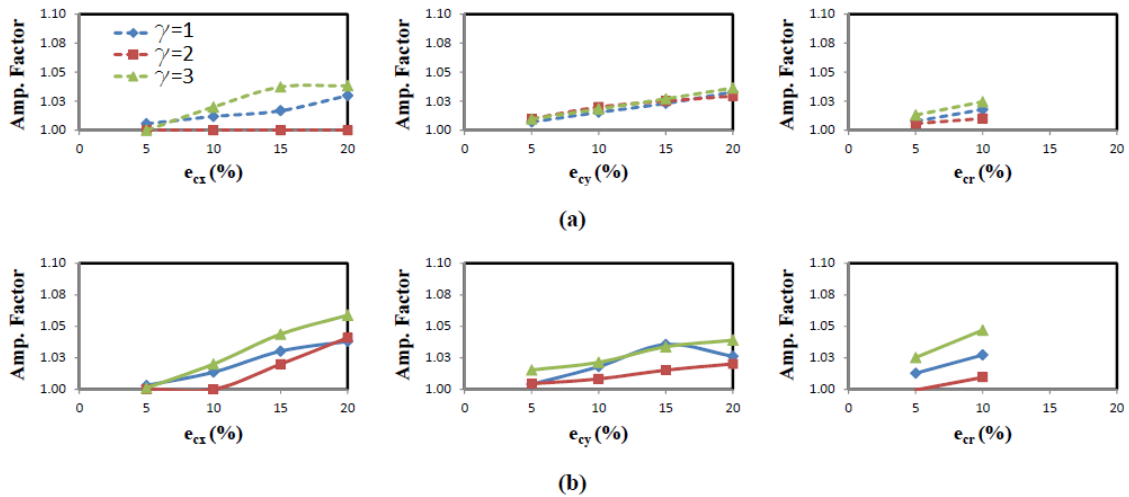


Fig. 4 Amplification Factor of isolator displacement in y direction for models with various γ ratios (a) XY components and (b) XYZ components

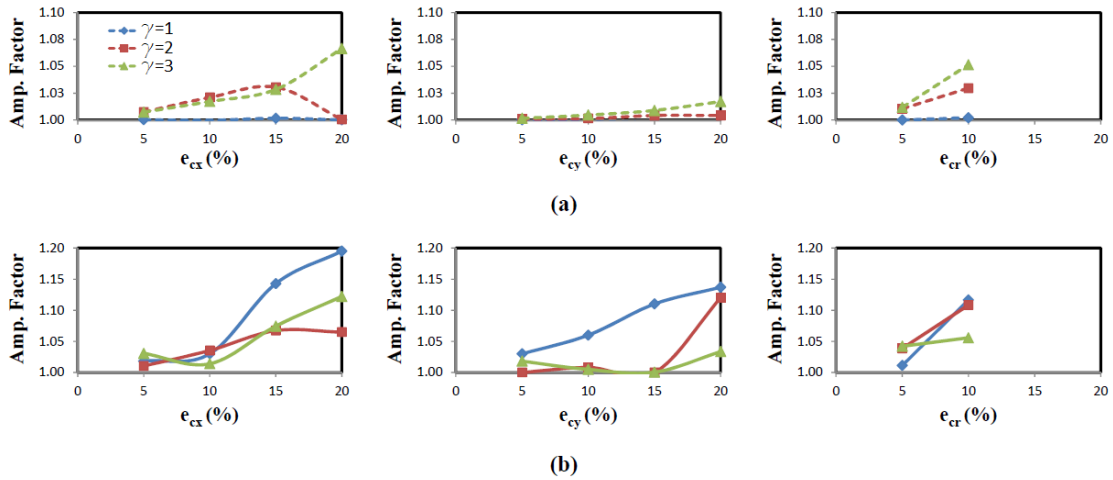


Fig. 5 Amplification Factor of base shear in y direction for models with various γ ratios (a) XY components and (b) XYZ components

direction in the case of the vertical component (XYZ) as illustrated in Fig. 4 are 1.068, 1.039 and 1.047 in longitudinal, transversal and diagonal eccentricities, respectively. Since mass eccentricity perpendicular to the direction of exerted force occurs in the path of torsion arm, it has the most effect on response increments. However, eccentricity in a route of force exerted does not have this impact. Also influence over diagonal eccentricity has been about the average effect of the longitudinal and transversal that seems reasonable. Due to all diagrams of this section, rate of response increment with presence of vertical component (XYZ) is more than the one in the state without the vertical component (XY), as it has been discussed precisely in chapter 6.

Amplification factor of base shear considering different eccentricities is shown in Fig. 5. As seen in the figure, by increasing eccentricity in three longitudinal, transversal and diagonal directions, value of response has also been added.

Peak amplification factor in a structure with $\gamma=1$ is 1.20, 1.13 and 1.10 for longitudinal, transversal and diagonal eccentricities, respectively.

Essential point in diagrams of base shear is that contrary to displacement amplification factors, effect of eccentricity on responses in the direction of exerted force is notable comparing with them in perpendicular trend. For instance, transversal eccentricity has increased the displacement less than 5 percent while it has amplified the base shear in y direction up to 12 percent. Main reason for this impact is that base shear of frictional isolated structures depends on the mass over them. Presence of eccentricity in the direction of exerted lateral force causes mass increment subjected to a number of isolators and decreased mass above the others comparing with symmetric case. Inequality of vertical force exerted on isolators also helps increase or decrease of the base shear that in general leads to escalation of the base shear of the structure.

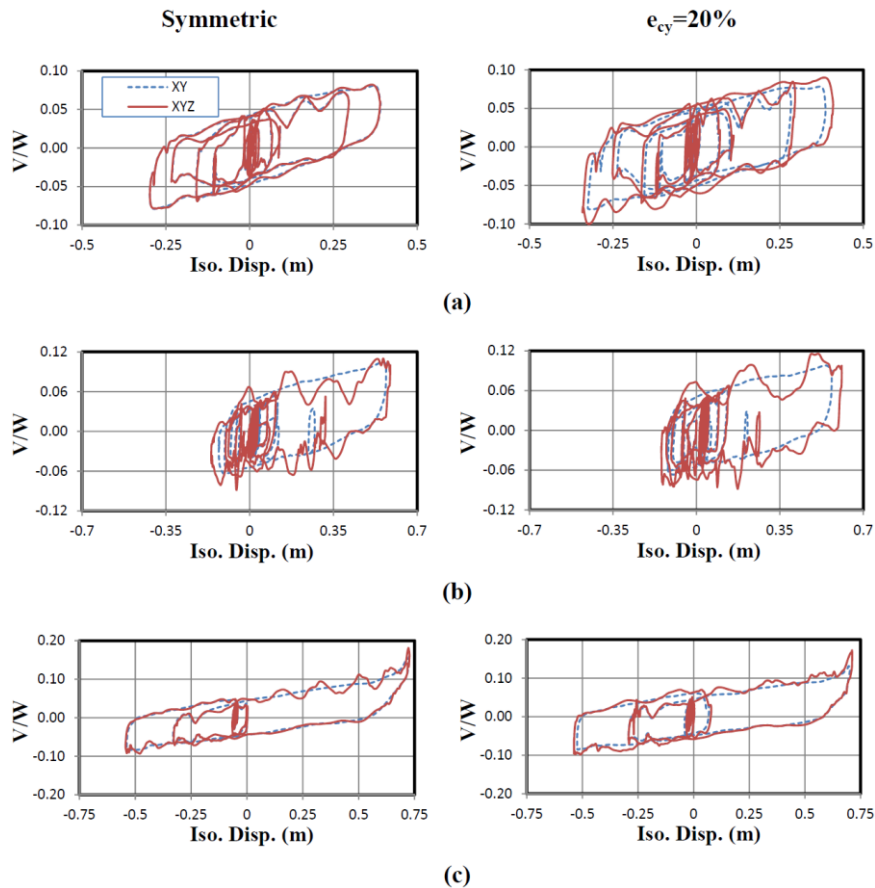


Fig. 6 Cyclic behavior of the structure in symmetric state $\gamma = 1$ and transversal eccentricity in y-direction (a) Duzce-Duzce, (b) Imperial Valley-Elcentro # 8 and (c) Kocaeli-Gebze earthquake

Vertical weight on the isolators has an additional effect on base shear diagrams that is the further increase in the amplification factor of smaller structures ($\gamma=1$) compared to longer ones ($\gamma=2$ & 3). While structures with fewer aspect ratios due to less superstructure weight have smaller base shear than the ones with greater aspects, they are more sensitive to the changes of mass eccentricity and in all diagrams of Fig. 5 amplification ratio has been declined by the increase of plan aspect. For example, as shown in the figure related to base shear of diagonal eccentricity $e_{cr}=10\%$, amplification factor in the presence of vertical component for structures with aspects of 1, 2 and 3 have been 1.12, 1.10 and 1.06, respectively.

One more thing to notice in the charts of the base shear is the vertical component's immense impact on the performance of mass eccentricity. The impact is to the extent that if the vertical component is increased, patterns of the figures will be changed and become similar to patterns seen in the diagrams of displacement amplification ratios. So by the absence of vertical component, effect of mass eccentricity on the base shear is very low.

Furthermore, increase of the plan aspect in most of the graphs has not changed the amplification factor significantly, but has increased it similar to the procedure in isolator displacement. The essential reason of the

difference between the diagrams of XYZ and XY is the dependence of base shear of frictional isolated structures on the upstanding force, as discussed before. The vertical effect also influenced the base shear by altering the weight amount exerted to TCFP bearings. Researchers have declared that the effect of vertical component on the base shear is 30% as well (Loghman *et al.* 2015a)

For better understanding the performance of isolator in the case of the vertical component and also mass eccentricity, cyclic behavior of a six-story structure with a square plan ($\gamma=1$) in the y-direction subjected to Duzce-Duzce, Imperial Valley-Elcentro # 8 and Kocaeli-Gebze earthquake records is shown in Fig. 6. In all diagrams existence of vertical component has led to swing of the base shear. This case states that in the points that vertical acceleration of earthquake gets its maximum, oscillations of base shear in cyclic motion has increased and lead to great changes of it. As it was explained previously, the effect of vertical component on the isolator displacement is small.

Increment of mass eccentricity in the diagrams of Fig. 6 with transversal eccentricity ($e_{cy}=20\%$) can lead to escalation in effect of the vertical component on isolator displacements; however, amount of the increase is essential for growth in the base shear and does not affect the displacement.

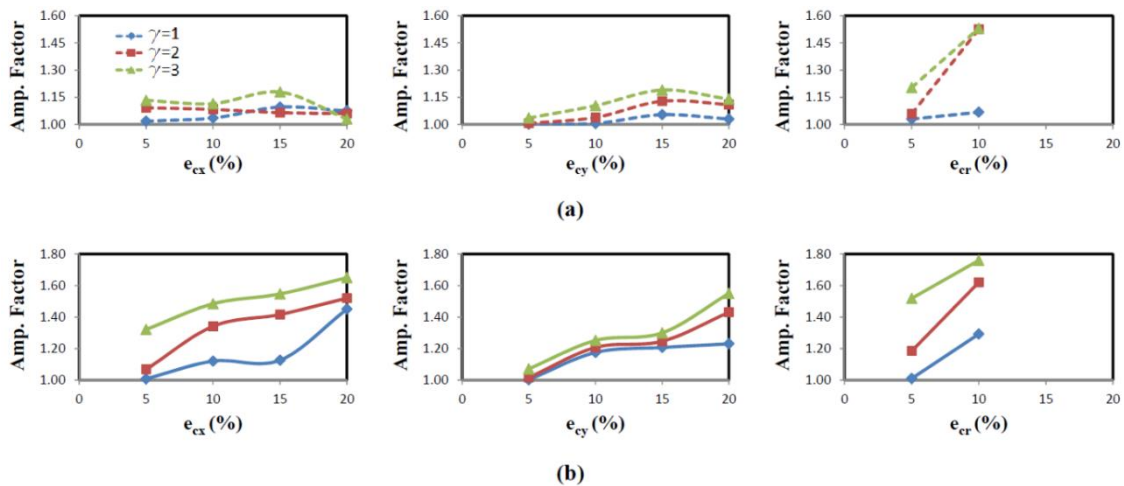


Fig. 7 Amplification factor of roof acceleration in y-direction in models with different γ ratios (a) XY components and (b) XYZ components

Influence procedure of mass eccentricity on roof acceleration of the superstructure in y-direction is illustrated in Fig. 7. The approaches seen in the graphs of the figure are almost similar to the displacement diagrams. However, rate of response increment is much greater than that graphs.

As illustrated in the diagrams of the figure related to the roof acceleration, the maximum amplification factor of the response of a structure with $\gamma=3$ is 1.65, 1.55 and 1.76 of XYZ and 1.18, 1.19 and 1.53 of XY state in the same order of longitudinal, transversal and diagonal eccentricities.

Effect of aspect of a structure (γ) on the response increment is remarkable as well as the displacement response. So, by increasing the aspect ratio of 1 to 3 in all diagrams, amplification factor of roof acceleration has been raised. Greater torsion arm of structure in rectangular structures than square ones, or better explained as more distance between centre of mass and the points on the corner of the plan which roof acceleration has been obtained from them, seems to be the most important factor in increase of the acceleration response.

In these graphs as well as the previous cases, considering the vertical component of an earthquake has affected the amplification factor of the roof. However, absence of it has not led to changes in amplification ratio patterns. Impact of vertical component on the roof acceleration and the reasons are explained more in chapter 6.

5.2 Slenderness Ratio (β)

Amplification factor of isolator displacement in the case of various eccentricities and in both XY and XYZ is similar to the results of Fig. 4 for structures with various γ ratios. Isolator displacement has not been changed a lot, so the maximum rate of increase in the 9-story building ($\beta=2$) with a longitudinal eccentricity equals to 1.057 in XYZ and 1.045 in XY state. Eccentricity in the direction perpendicular to the direction investigated has the most impact on raising displacement response as well as what is resulted in chapter 5.1 of this study.

Effect of mass eccentricity on base shear of structures with different slenderness ratios is illustrated in Fig. 8. Longitudinal and transversal eccentricities equal to 20% have caused 1.224 and 1.243 increase (almost the same value) in base shear of the 3-story structure. However, diagonal eccentricity of 15% has raised it to 1.751, which proves that diagonal eccentricity or more precisely, simultaneous presence of both longitudinal and transversal eccentricity can intensify the impact on base shear.

Effect of increasing mass eccentricity on amplification factor of base shear for short-rise isolated buildings (3-story) is much more than medium ones (6- and 9-story) as mentioned in Fig. 8. For example, by growing slenderness ratio of 0.67 to 2 in diagonal eccentricity of 15% ($e_{cr}=15\%$) amplification factor declined from 1.751 to 1.124. The most essential reason for this result, as discussed in structures with different aspect factor, is less base shear of short structures and therefore being more sensitive to changes in the base shear caused by vertical load on the isolator.

It is also shown in the diagrams that presence or absence of the vertical component has a significant influence on the changes of base shear. So in the absence of vertical component, amplification factor of the response dropped from 1.751 to 1.04. In other words, if the analysis is done without vertical component, effect of mass eccentricity on increasing base shear and isolator displacement can be ignored with no trouble.

The most important reason for little impact of torsion caused by mass eccentricity on isolator displacement and also base shear with no consideration of the vertical component is the ability of TCFP bearing to control huge movements. This ability is due to two hardening phases that are created in the end of motion diagram of the bearing (phase IV and V). For instance, two diagrams compared in Fig. 6(c) can be considered. In the figure, 20% transversal eccentricity cannot make significantly changes in displacement and therefore base shear of isolator. Since isolator reaches its final capacity of displacement, there

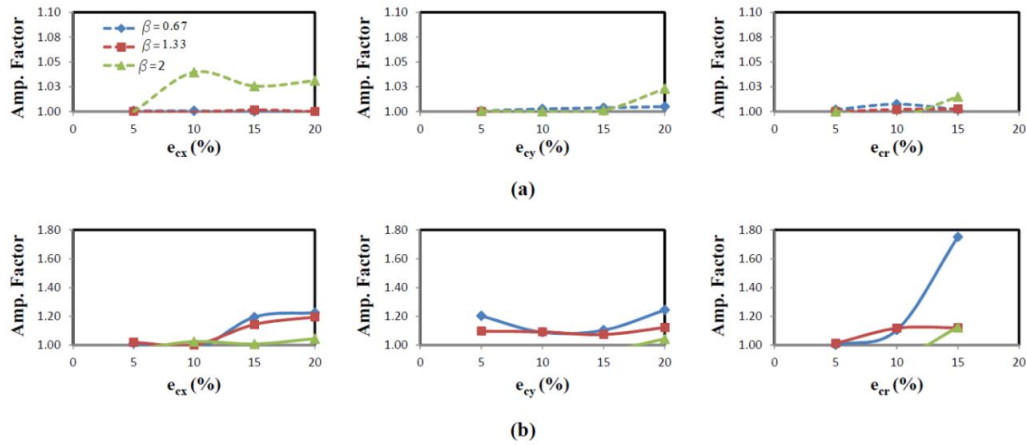


Fig. 8 Amplification Factor of base shear in y-direction for models with different β ratios (a) XY components and (b) XYZ components

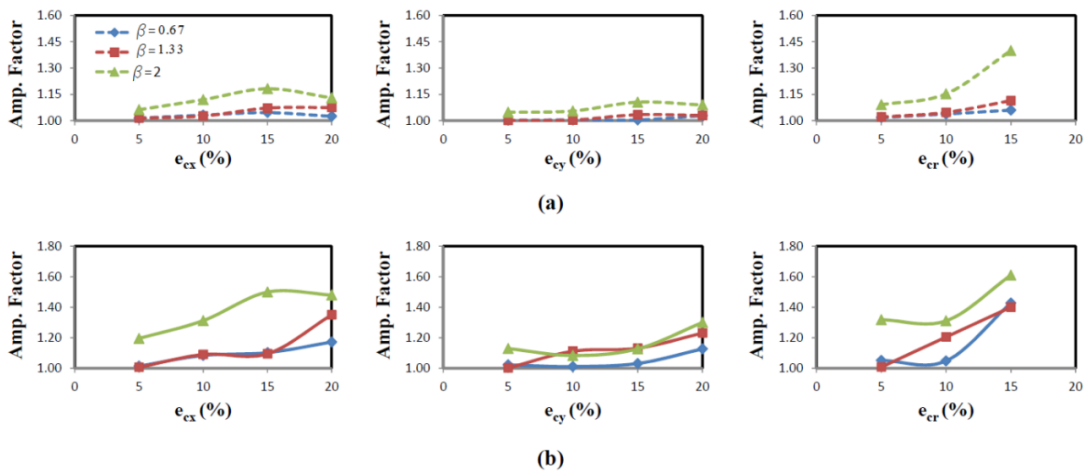


Fig. 9 Amplification factor of roof acceleration in y-direction for models with different β ratios (a) XY components and (b) XYZ components

is no place for more deformations. And also amplification factor of base shear approximately equals to the factor of isolator displacement in the absence of the vertical component, as discussed before.

Mass eccentricity also affects roof acceleration of the superstructure that is shown in Fig. 9. Trends seen in diagrams of the figure are very similar to the way that displacement has changed, although rate of increase here is much larger than the one in the displacement response. As seen in the corresponding graphs, peak amplification factor of the structure with slenderness ratio of 2 ($\beta=2$) in longitudinal, transversal and diagonal directions in the case of the vertical component (XYZ) is 1.48, 1.3 and 1.61 and in the absence of it, is 1.13, 1.09 and 1.40 in the same order.

Amplification factor of the response has been larger in the structures with longitudinal eccentricity (e_{cx}) than in the state of transversal eccentricity (e_{cy}). As previously discussed, being perpendicular to the movement direction and rise in torsion arm in the plan, has caused responses to be greater in x-direction. Also diagonal eccentricity makes responses grow, since it includes both types of eccentricities.

Increase in slenderness ratio of the structure has led to growth in amplification factor of acceleration seen in most of the diagrams of Fig. 9. For example, considering transversal eccentricity of 20% amplification factor in the case of vertical component (XYZ) has increased from 1.126 to 1.30 by rising slenderness ratio of 0.67 to 2, in other words rising stories from 3 to 9. The important reason for this fact is increase in structure's acceleration by the growth in number of stories. While acceleration in stories raises in tall buildings because of relative drift of them, it is obvious that in a structure with great number of stories we will face with great accelerations. Although acceleration of stories in isolated structures is very low comparing with fixed-support-structures, this much low value is increased by raising height of structure. In diagrams of Fig. 9 like previous figures the vertical component has effected roof acceleration remarkably; however, absence of it has not altered the pattern of changes in amplification factor.

Table 3 Properties of different TCFP isolators

Design	T_{eff} (sec)	ξ_{eff} (%)	Displacement Capacity-D			Effective Radii- R_{eff}		Friction Coefficient- μ		
			$d_1=d_4$	$d_2=d_3$	D(Total)	$R_{\text{eff1}}=R_{\text{eff4}}$	$R_{\text{eff2}}=R_{\text{eff3}}$	$\mu_2=\mu_3$	μ_1	μ_4
TCFP-1	3	15	0.45	0.05	1.0	2.0	0.3	0.05	0.115	0.2
TCFP-2	4	15	0.45	0.05	1.0	3.5	0.3	0.02	0.06	0.11
TCFP-3	5	15	0.45	0.05	1.0	5.5	0.45	0.02	0.04	0.07
TCFP-4	5	10	0.45	0.05	1.0	5.5	0.45	0.02	0.025	0.06
TCFP-5	5	20	0.45	0.05	1.0	5.5	0.45	0.02	0.06	0.07

5.3 Isolator properties

In all previous results, the TCFP isolator with effective period of 5 second and damping ratio of 15% has been used. In order to expand the results obtained from this particular isolator to all TCFP isolators, it's necessary to take a look at the affection of changes of isolators on the responses of various structures. Therefore the superstructure with a square plan and 6 stories ($\gamma=1$, $\beta=1.33$) placed on different types of isolator designed with parameters of Table 3 and analyzed under 25 earthquakes shown in Table 1 in both XY and XYZ cases. The average amplification factor of responses for displacement and base shear in y-direction for the superstructure supported by isolators with different T_{eff} and ξ_{eff} is presented in this chapter. Results in this chapter have been illustrated only in transversal eccentricity (e_y).

According to the results for isolators with different periods, the amplification factor for the displacement of all the models is less than 1.1, therefore, the graphs are not presented here. But it should be noted that generally in an isolator with higher period the displacement is more; and the isolator goes through its hardening levels or phases IV or V, therefore limited displacement variations as a result of hardening movement graphs are obvious. In other words, hardening affection which is a crucial specification of TCFP isolators plays a role in isolators with high effective periods. Vice versa what mentioned previously, in higher phases of movement because of hardening in the diagram of force-displacement increasing the mass eccentricity leads to enhance base shear more than growth of the displacement and this increment is less in lower movement phases than higher ones. This issue is obviously specified in Fig. 10. In isolators with effective period of 3, 4 and 5 seconds, the maximum amplification factors in transversal eccentricity are 1.031, 1.123 and 1.121, respectively. Also it should be considered that in these diagrams the affection of vertical component of earthquake on increasing of the base shear is negligible as well as the prior two states (different aspect and slenderness ratio, see section 5.1 and 5.2), so that it can be claimed that in the case of existence of only horizontal components of earthquake (XY), the influence of mass eccentricity on all types of isolators is negligible.

Similar to displacement results, the shorter period of isolator causes higher amplification factor of roof acceleration in Fig. 10, because the shorter-period bearings behave in stiffening phases i.e. phases I to III and torsion makes them show greater responses. In addition, presence of vertical component of ground motion increases the acceleration Amp Factor from 1.48 to 2 in a model

supporting on 3-seconds-period isolator experiencing 20% mass eccentricity in transversal direction.

In the graphs of Fig. 11 variations of isolator base shear and roof acceleration of isolated structure with effective period of 5 seconds and damping ratios of 10 to 20% are displayed. In the results obtained, isolators with low damping ratio show great amplification factors of base shear. For instance, peak amplification factor of base shear for longitudinal, transversal and diagonal eccentricities with damping ratio of 10% is 1.602, 1.803 and 1.404, as the same order. A glance at the behavioral graph of isolators with different damping ratios can prove the reason of this increase. If the displacement capacity and effective periods of TCFP isolators were constant, isolators with low damping ratios would have greater stiffness in all of their phases of movement than the ones with high damping ratios. So in general, their base shear is large. That is why by occurrence of torsion due to eccentricity, base shear increase is also great in these isolators.

6. Effects of vertical component of earthquake

According to the results of chapter 5, vertical component is a crucial parameter in amplifying the base shear and roof acceleration responses. For better comprehending of this subject, effect of vertical component of ground motion is studied specifically for symmetric structures to avoid influence of torsion caused by eccentricity in other models. In this sections' table and curves, ratios of responses are normalized in the case of the vertical component (XYZ) to the absence of it (XY) according to Eq. (2) and the average values are displayed in both x and y directions for 25 earthquake records shown in Table 1.

Rate of increase of y-direction structure responses with different aspect and slenderness ratios as well as isolators with various properties are displayed in Table 4. Values of base shear of the structures investigated in this table for aspect ratios of 1 to 3 have been increased about 1.18 to 1.35, respectively considering the vertical component. As already mentioned, base shear of structures rested on frictional isolators is highly dependent on the vertical force exerted on them; therefore, the vertical component that causes a lot of changes in structure's mass can help to raise it. In addition, the larger structural dimensions in plan, the more increasing effect of the vertical component on the base shear. Changing a square plan to a rectangular one has ascending results in base shear, as well.

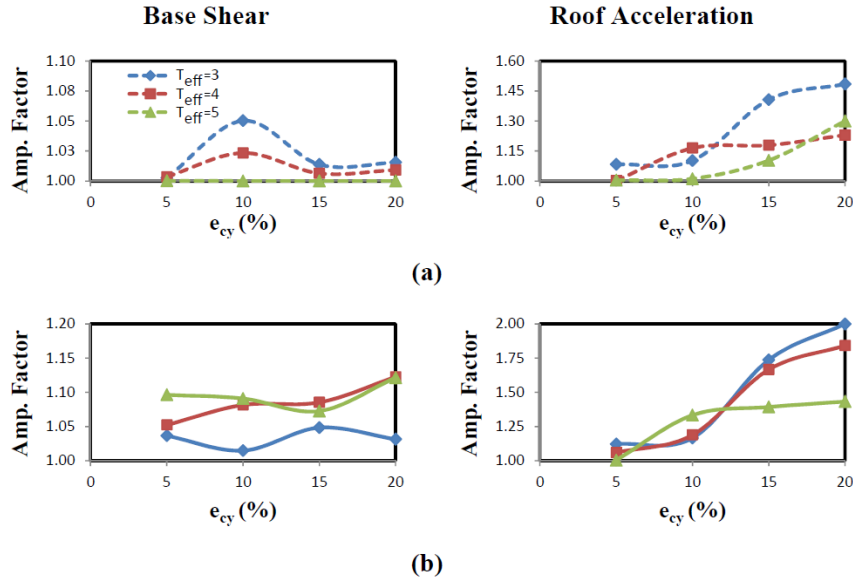


Fig. 10 Amplification factor of base shear and roof acceleration in y-direction of models with different T_{eff} caused by transversal eccentricity (a) XY components and (b) XYZ components

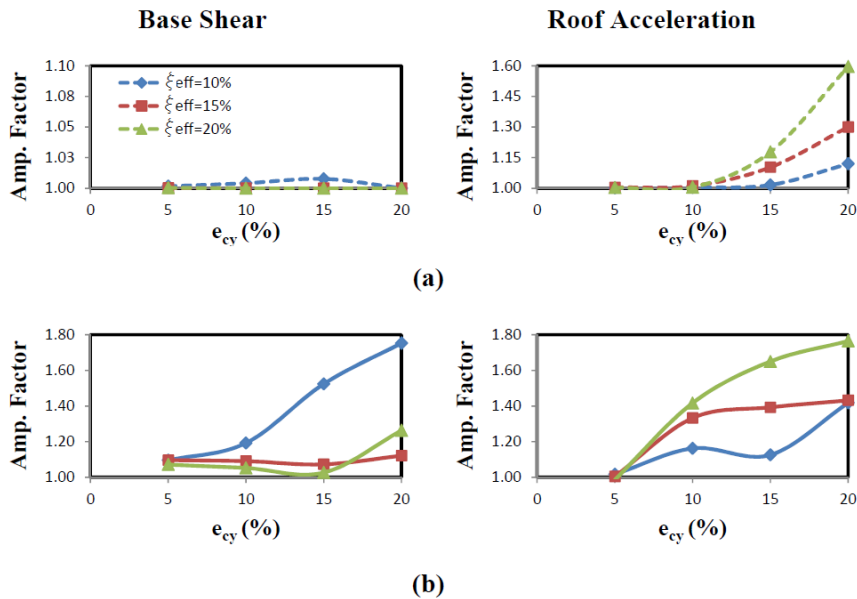


Fig. 11 Amplification factor of base shear and roof acceleration in y-direction of models with different xi_{eff} caused by transversal eccentricity (a) XY components and (b) XYZ components

The maximum roof acceleration of all models with aspect ratios of 1 to 3 has significantly raised considering the vertical component of earthquakes. Maximum acceleration ratio in the case of the vertical component (XYZ) to the absence of it (XY) is 1.66. To clarify how roof acceleration grows in the presence of the vertical component of ground motion, acceleration time history graph in y-direction with a square plan ($\gamma = 1$) for 3 earthquakes including Duzce-Duzce, Imperial Valley-Elcentro # 8 and Kocaeli-Gebze is displayed in Fig. 12. Diagrams present a comparison between the acceleration in

the case of vertical component (XYZ) to the absence of it (XY).

As shown in all diagrams of Fig. 12 presence of the vertical component has increased not only maximum roof acceleration but also acceleration in most parts of the graph. According to the behavioral diagrams of TCFP isolators in all five phases of motion that has been introduced in chapter 1 of this study, stiffness of all phases has a direct relationship

$$XYZ / XY = \frac{RESPONSE (XYZ \text{ case})}{RESPONSE (XY \text{ case})} \quad (2)$$

Table 4 XYZ/XY ratio for base shear and roof acceleration of symmetric models

Response:	Base Shear			Roof Acceleration		
Aspect Ratio (γ)	1	2	3	1	2	3
XYZ/XY Ratio	1.18	1.33	1.35	1.66	1.55	1.46
Slenderness Ratio (β)	0.67	1.33	2	0.67	1.33	2
XYZ/XY Ratio	1.21	1.18	1.26	1.22	1.66	1.67
Isolator Period (T_{eff})-s	3	4	5	3	4	5
XYZ/XY Ratio	1.23	1.23	1.18	1.17	1.29	1.66
Isolator Damping (ξ_{eff})-%	10	15	20	10	15	20
XYZ/XY Ratio	1.20	1.18	1.21	1.66	1.66	1.40

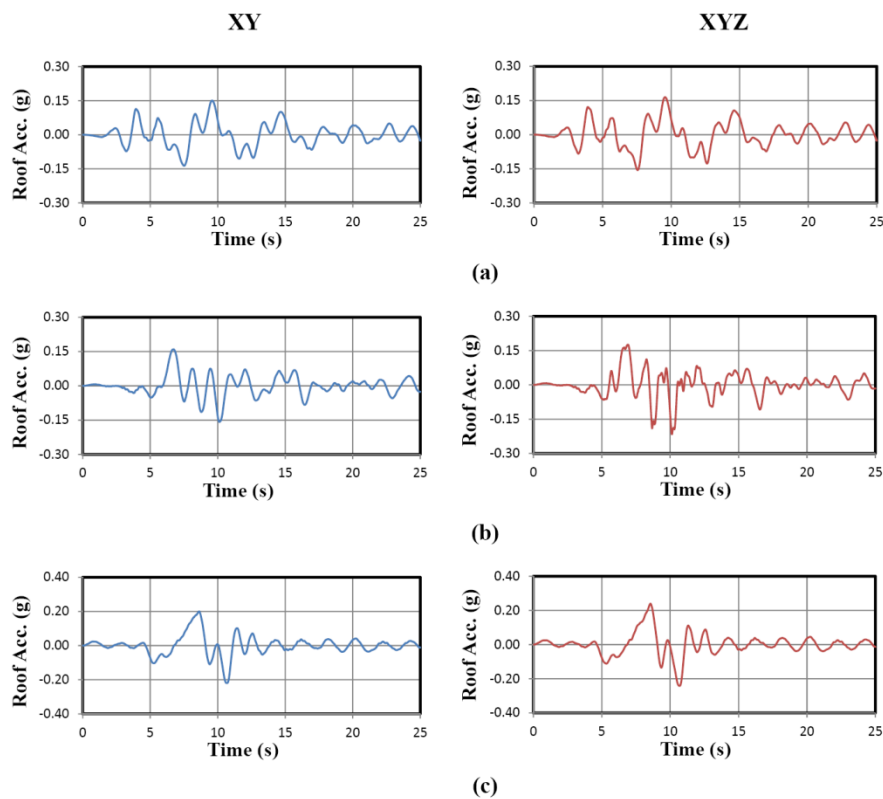


Fig. 12 Roof acceleration time history with and without vertical component in y-direction of the structure with $\gamma = 1$ (a) Duzce-Duzce, (b) Imperial Valley-Elcentro # 8 and (c) Kocaeli-Gebze earthquake

with the vertical weight on the isolator (W). When vertical acceleration subjects upward to the building during the earthquake, diminishing weight on the isolator decreases its hardness. Thus acceleration and displacement grows at that moment. Because of some restrictions on displacement of isolators, it's not possible that displacements exceed design limitations; however, there is no limitation on the roof acceleration and its value is easily increased. Due to the XY diagrams in Fig. 12, it should be considered that in isolated-structures acceleration is greatly reduced because of reduction in the amount of force exerted on them. For example, the maximum acceleration is less than 0.2 g in XY position shown in diagrams of Fig. 12. Therefore, obviously

a slight increase in the amount of acceleration in the case of vertical component causes a large quotient of acceleration in XYZ to XY case. Increasing responses of the structures with different slenderness ratio (β) in the presence of vertical component is shown in Table 4 as well. The effect of the vertical component on base shear as seen in the table is about 20%. Also the vertical component of earthquake has raised acceleration in y-direction 1.22 and 1.67 times respectively in three-story and nine-story structure and it seems logical due to the larger number of stories of the second structure than the first one.

The impact of the vertical component on the response of the six-story structure with a square plan ($\gamma=1$, $\beta=1.33$) and

supported on isolators with different effective period and damping is investigated in Table 4. Results in the table indicate that isolator specifications do not affect growth in the base shear in the case of the vertical component. However, the vertical component remarkably affects roof acceleration of the structures rested on isolators with high effective period (5 seconds) and damping ratio (20 percent) that have less stiffness in the behavioral diagram of TCFP than the rest.

7. Conclusions

In the current study, effect of vertical as well as horizontal components of near-field earthquakes has been investigated on asymmetric isolated structures. Superstructures with 3, 6 and 9 stories with length to width ratios of 1, 2 and 3 in plan and linear elastic models have been studied. TCFP isolators have effective period of 3 to 5 and damping ratio of 10 to 20 percent and modeling of them has been done in nonlinear state. Mass eccentricity of the superstructure in length, width and diameter of the plan has been considered and the amplification factor value influenced by torsion in the various responses of the structure has been obtained. Also importance of the impact of the vertical component of earthquake on the response of the structure has caused to separately investigate this effect on symmetric structures. Results have been obtained from the study as below:

- By the increase of aspect ratio and changing square plan to rectangular, effect of mass eccentricity on isolator displacement and roof acceleration has been raised and decreased in base shear. In structures with different γ maximum amplification factor of displacement and acceleration response have been respectively 1.08 and 1.65 in a structure with length to width ratio of 3 in plan and maximum base shear increment has been in the structure with aspect ratio of 1 and the value of 1.2.
- By the increase of β ratio and height, effect of mass eccentricity on base shear is reduced. The most important reason for this issue is the dependence of the base shear of frictional isolators on the vertical force exerted to them. For example, amplification factor of the response of base shear in a three-story structure has been 1.75 and 1.12 in a nine-story one.
- By escalation of the number of stories and the slenderness ratio, amplification factor of roof acceleration significantly has been increased so that in the nine-story structure has reached to 1.61.
- In all studied models, eccentricity in the direction of the subjected earthquake has the most impact on base shear. However, isolator displacement and roof acceleration has mostly influenced by the eccentricity perpendicular to the earthquake path.
- Changes of isolator specifications have not affected the displacement response growth; however, by increasing the effective period

amplification factor of base shear has been raised and by rising effective damping ratio, the response has been reduced.

- In all cases discussed in this study, effect of the vertical component on the responses of structures with mass asymmetries, especially on the base shear, has been remarkable. Influence of this component on base shear is to some extent that can be claimed that in the absence of the vertical component, mass eccentricity has a little effect on the base shear increase.

In a symmetric structure, presence of vertical component of earthquake has no sensible effect on isolators' displacements but it can raise base shear up to 1.35 times. Impact of this component on acceleration is also remarkable so that it has increased the roof acceleration of a nine-story structure 1.67 times, compared to the case only two horizontal components.

References

- AISC (2010), "Seismic provisions for structural steel buildings", ANSI/AISC 341-10, American Institute of Steel Construction, Chicago, Illinois, USA.
- AISC (2010), "Specification for structural steel buildings", ANSI/AISC 360-10, American Institute of Steel Construction, Chicago, Illinois, USA.
- Almazan, J.L., De la llera, J.C. and Inaudi, J.A. (1998), "Modeling aspects of structures isolated with the frictional pendulum system", *Earthq. Eng. Struct. D.*, **27**(80), 845–867.
- Almazan, J.L. and De la llera, J.C. (2003), "Accidental torsion due to overturning in nominally symmetric structures isolated with the FPS", *Earthq. Eng. Struct. D.*, **32**, 919-948.
- ASCE 7-10 (2010), "Minimum Design Loads for Building and Other Structures", ASCE/SEI 7-10, American Society of Civil Engineers, Reston, Virginia, USA.
- Ates, S. and Yurdakul, M. (2011), "Site-response effects on RC buildings isolated by triple concave friction pendulum bearings", *Comput. Concrete*, **8**(6), 693–715.
- Becker, T.C. and Mahin, S.A. (2012), "Experimental and analytical study of the bi-directional behavior of the triple friction pendulum isolator", *Earthq. Eng. Struct. D.*, **41**, 355-373.
- Becker, T.C. and Mahin, S.A. (2013), "Approximating peak responses in seismically isolated buildings using generalized modal analysis", *Earthq. Eng. Struct. D.*, **42**, 1807-1825.
- Constantinou, M.C., Kalpakidis, I., Filiatrault, A. and Ecker Lay, R.A. (2011), "LRFD-based analysis and design procedures for bridge bearings and seismic isolation", Technical Report MCEER-11-0004, State University of New York at Buffalo, Buffalo, New York, USA.
- Dao, N.D., Ryan, K.L., Sao, E. and Sasaki, T. (2013), "Predicting the displacement of triple pendulum bearings in a full-scale shaking experiment using a three-dimensional element", *Earthq. Eng. Struct. D.*, **42**, 1677-1695.
- De la llera, J.C. and Almazan, J.L. (2003), "An experimental study of nominally symmetric and asymmetric structures isolated with the FPS", *Earthq. Eng. Struct. D.*, **32**, 891-918.
- De la llera, J.C. and Chopra, A.K. (1994), "Accidental torsion in buildings due to base rotational excitation", *Earthq. Eng. Struct. D.*, **23**, 1003-1021.
- Dicleli, M. and Buddaram, S. (2007), "Equivalent linear analysis of seismic-isolated bridges subjected to near-fault ground motions with forward rupture directivity effect", *Eng. Struct.*,

- 29, 21-32.
- Dicleli, M. (2007), "Supplemental elastic stiffness to reduce isolator displacements for seismic-isolated bridges in near-fault zones", *Eng. Struct.*, **29**, 763-775.
- Fadi, F. and Constantinou, M.C. (2010), "Evaluation of simplified methods of analysis for structures with triple friction pendulum isolators", *Earthq. Eng. Struct. D.*, **39**(1), 5-22.
- Fenz, D. and Constantinou, M.C. (2008a), "Mechanical behavior of multi-spherical sliding bearings", Technical Report No. MCEER-08/0007, State University of New York at Buffalo, Buffalo, New York, USA.
- Fenz, D. and Constantinou, M.C. (2008b), "Modeling triple friction pendulum bearings for response history analysis", *Earthq. Spectra*, **24**, 1011-1028.
- Jangid, R.S. and Datta, T.K. (1995), "Performance of base isolation systems for asymmetric building subjected to random excitation", *Eng. Struct.*, **17**(6), 443-454.
- Jangid, R.S. and Kelly, J.M. (2001), "Base isolation for near-fault motions", *Earthq. Eng. Struct. D.*, **30**, 691-707.
- Jangid, R.S. (2005), "Optimum friction pendulum system for near-fault motions", *Eng. Struct.*, **27**, 349-359.
- Khoshnoudian, F. and Ahmadi, E. (2013), "Effects of pulse period of near-field ground motions on the seismic demands of soil-MDOF structure systems using mathematical pulse models", *Earthq. Eng. Struct. D.*, **42**(11), 1565-1582.
- Khoshnoudian, F. and Imani Azad, A. (2011), "Effect of two horizontal components of earthquake on nonlinear response of torsionally coupled base isolated structures", *Struct. Des. Tall Spec. Build.*, **20**, 986-1018.
- Khoshnoudian, F. and Rabiei, M. (2010), "Seismic response of double concave friction pendulum base-isolated structures considering vertical component of earthquake", *Adv. Struct. Eng.*, **13**(1), 1-13.
- Khoshnoudian, F. and Rezai Haghdoost, V. (2009), "Responses of pure-friction sliding structures to three components of earthquake excitation considering variations in the coefficient of friction", *Scientia Iranica, Transaction A: Civil Engineering*, **16**(6), 429-442.
- Kilar, V. and Koren, D. (2009), "Seismic behaviour of asymmetric base isolated structures with various distributions of isolators", *Eng. Struct.*, **31**, 910-921.
- Loghman, V. and Khoshnoudian, F. (2015) "Comparison of seismic behavior of long period SDOF systems mounted on friction isolators under near-field earthquakes", *Smart Structures and Systems*, Accepted in Press.
- Loghman, V., Khoshnoudian, F. and Banazadeh, M. (2015a), "Effects of vertical component of earthquake on seismic responses of triple concave friction pendulum base-isolated structures", *J. Vib. Control*, **21**(11), 2099-2113.
- Loghman, V., Tajammolian, H. and Khoshnoudian, F. (2015b), "Effects of rotational components of earthquakes on seismic responses of triple concave friction pendulum base-isolated structures", *J. Vib. Control*, DOI: 10.1177/1077546315594066.
- Masaeli, H., Khoshnoudian, F. and Hadikhan Tehrani, M. (2014), "Rocking isolation of nonductile moderately tall buildings subjected to bidirectional near-fault ground motions", *Eng. Struct.*, **80**, 298-315.
- Morgan, T. and Mahin, S.A. (2010), "Achieving reliable seismic performance enhancement using multi-stage friction pendulum isolators", *Earthq. Eng. Struct. D.*, **39**, 1443-1461.
- Morgan, T.A. and Mahin, S.A. (2011), "The use of base isolation systems to achieve complex seismic performance objectives", Report No. PEER-2011/06, Pacific Earthquake Engineering Research Center (PEER), Berkeley, CA, USA.
- Panchal, V.R. and Jangid, R.S. (2008), "Variable friction pendulum system for near-fault ground motions", *Struct. Control Health Monit.*, **15**, 568-584.
- PEER (2013), "PEER ground motion database", development by the Pacific Earthquake Engineering Research Center (PEER), <http://ngawest2.berkeley.edu>
- Picazo, Y., Lopez, O.D. and Esteva, L. (2015), "Seismic reliability analysis of buildings with torsional eccentricities", *Earthq. Eng. Struct. D.*, **44**, 1219-1234.
- Rabiei, M. and Khoshnoudian, F. (2011), "Response of multi-story friction pendulum base-isolated buildings including the vertical component of earthquake", *Canadian J. Civil Eng.*, **38**, 1045-1059.
- Rabiei, M. and Khoshnoudian, F. (2013), "Seismic response of elevated liquid storage tanks using double concave friction pendulum bearings with tri-linear behavior", *Adv. Struct. Eng.*, **16**(2), 315-338.
- Roussis, P.C. and Constantinou, M.C. (2006a), "Uplift-restraining friction pendulum seismic isolation system", *Earthq. Eng. Struct. D.*, **35**, 577-593.
- Roussis, P.C. and Constantinou, M.C. (2006b), "Experimental and analytical studies of structures seismically isolated with an uplift-restraining friction pendulum system", *Earthq. Eng. Struct. D.*, **35**, 595-611.
- Ryan, K.L. and Chopra, A.K. (2006), "Estimating bearing response in symmetric and asymmetric-plan isolated buildings with rocking and torsion", *Earthq. Eng. Struct. D.*, **35**, 1009-1036.
- Sarlis, A.A. and Constantinou, M.C. (2013), "Model of triple friction pendulum bearing for general geometric and frictional parameters and for uplift conditions", Report No. MCEER-13-0010, State University of New York at Buffalo, Buffalo, New York, USA.
- Siringurino, D.M. and Fujino, Y. (2015), "Seismic response analyses of an asymmetric base-isolated building during the 2011 Great East Japan (Tohoku) Earthquake", *Struct. Control Health Monit.*, **22**, 71-90.
- Tajammolian, H., Khoshnoudian, F., Talaei, S. and Loghman, V. (2014), "The effects of peak ground velocity of near-field ground motions on the seismic responses of base-isolated structures mounted on friction bearings", *Earthq. Struct.*, **7**(6), 1259-1282.
- Tajammolian, H., Khoshnoudian, F. and Bokaeian, V. (2016b), "Seismic responses of asymmetric steel structures isolated with the TCFP subjected to mathematical near-fault pulse models", *Smart Struct. Syst.*, **18**(5), 931-953.
- Tajammolian, H., Khoshnoudian, F. and Partovi Mehr, N. (2016a), "Seismic responses of isolated structures with mass asymmetry mounted on TCFP subjected to near-fault ground motions", *Int. J. Civil Eng.*, DOI: 10.1007/s40999-016-0047-9
- Tena-Colunga, A. and Escamilla-Cruz, J. (2007), "Torsional amplifications in asymmetric base isolated structures", *Eng. Struct.*, **29**(2), 237-247.
- Tena-Colunga, A. and Gomez-Soberon, L. (2002), "Torsional response of base isolated structures due to asymmetries in the superstructure", *Eng. Struct.*, **24**, 1587-1599.
- Tena-Colunga, A. and Zambrana-Rojas, C. (2006), "Dynamic torsion amplifications in asymmetric base isolated structures with an eccentric isolation system", *Eng. Struct.*, **28**(3), 72-83.
- Yurdakul, M. and Ates, S. (2011), "Modeling of triple concave friction pendulum bearings for seismic isolation of buildings", *Struct. Eng. Mech.*, **40**(3), 315-334.
- Zayas, V.A., Low, S.S., Bozzo, L. and Mahin, S.A. (1989), "Feasibility and performance studies on improving the earthquake resistance of new and existing buildings using the friction pendulum system", Report No. UCB/EERC-89/09, Earthquake Engineering Research Center, University of California Berkeley, Berkeley, CA, USA.
- Zayas, V.A., Low, S.S. and Mahin, S.A. (1987), "The SFP earthquake resisting system: experimental report", Report No.

UCB/EERC-87/01, Earthquake Engineering Research Center,
University of California Berkeley, Berkeley, CA, USA.

CC